Nucleation and Growth of Ice Crystals Inside Cultured Hepatocytes During Freezing in the Presence of Dimethyl Sulfoxide

Jens O. M. Karlsson,* Ernest G. Cravalho,* Inne H. M. Borel Rinkes,‡ Ronald G. Tompkins,‡ Martin L. Yarmush,‡§ and Mehmet Toner‡

‡Surgical Research Laboratory, Massachusetts General Hospital, and Shriners Burns Institute, and Department of Surgery, Harvard Medical School, Boston, Massachusetts 02114; *Department of Mechanical Engineering, Massachusetts Institute of Technology, Cambridge, Massachusetts 02139; and §Department of Chemical and Biochemical Engineering, Rutgers University, Piscataway, New Jersey 08885 USA

ABSTRACT A three-part, coupled model of cell dehydration, nucleation, and crystal growth was used to study intracellular ice formation (IIF) in cultured hepatocytes frozen in the presence of dimethyl sulfoxide (DMSO). Heterogeneous nucleation temperatures were predicted as a function of DMSO concentration and were in good agreement with experimental data. Simulated freezing protocols correctly predicted and explained experimentally observed effects of cooling rate, warming rate, and storage temperature on hepatocyte function. For cells cooled to −40°C, no IIF occurred for cooling rates less than 10°C/min. IIF did occur at faster cooling rates, and the predicted volume of intracellular ice increased with increasing cooling rate. Cells cooled at 5°C/min to −80°C were shown to undergo nucleation at −46.8°C, with the consequence that storage temperatures above this value resulted in high viability independent of warming rate, whereas colder storage temperatures resulted in cell injury for slow warming rates. Cell damage correlated positively with predicted intracellular ice volume, and an upper limit for the critical ice content was estimated to be 3.7% of the isotonic water content. The power of the model was limited by difficulties in estimating the cytosol viscosity and membrane permeability as functions of DMSO concentration at low temperatures.

INTRODUCTION

Although the development of hepatocyte-based bioartificial liver devices still faces many challenges, these devices seem to represent the most promising approach for the replacement of normal liver function (Yarmush et al., 1992). Although efficient methods for procuring and maintaining hepatocytes in long-term culture exist, technologies for preserving them are lagging behind. To realize their full clinical potential, isolated and/or cultured hepatocytes will need to be preserved for significant periods of time so that they can be appropriately banked and distributed on demand. Efforts have been directed toward warm and cold storage in tissue culture medium; but, because of the expense of storage, the likelihood of contamination, and the relatively short-term survival of the stored tissue, cryopreservation has become the preservation technique of choice.

The majority of studies on hepatocyte cryopreservation have involved the use of freshly isolated rat hepatocytes in suspension (Fuller et al., 1983; Gomez-L. et al., 1984; Novicki et al., 1982). It has been shown that the process of freezing and thawing inflicts considerable damage on the isolated hepatocytes (Chesné and Guillouzo, 1988; Fuller et al., 1983; Innes et al., 1988; Rijntjes et al., 1986). In many cases, the results (which are generally short-term) are contradictory and depend largely on the methods used for the assessment of viability. There are also a few reports concerning cryopreservation of cultured hepatocytes (Hubel et al., 1991; Yarmush et al., 1992). Recently, we have developed a cryopreservation protocol for rat hepatocytes cultured in a sandwich configuration which resulted in a ~75% recovery of long-term protein secretion and morphology for at least 2 weeks after freezing to −80°C (Borel Rinkes et al., 1992b). Although long-term post-thaw function was demonstrated in this study, further work is clearly needed to develop a fundamental understanding of the physicochemical processes occurring during freezing of cultured hepatocytes.

Because experimental evidence suggests a correlation between intracellular ice formation (IIF) and cell injury for many cell types (Mazur, 1984), cryobiologists have sought to better understand both the IIF process and the mechanism by which it causes cell damage. We have previously developed a model of heterogeneous ice nucleation and water transport which has been successful in predicting the likelihood of IIF in hepatocytes (Toner et al., 1992). The potential of this model as a design tool for cryopreservation protocols has been demonstrated by Toner et al. (1993), who used their predictions to optimize a nonequilibrium freezing protocol for mouse embryos. However, this original model is applicable only to cell freezing in the absence of cryoprotective additives (CPAs). Because CPAs are almost ubiquitous in cryopreservation, this limitation of the model must be addressed. Pitt and co-workers, taking a phenomenological approach to the problem of predicting ice formation in cells, have developed a stochastic model that incorporates the effects of cooling rate, CPAs, and other factors on the probability of IIF (Pitt, 1992). Compared with mechanistic approaches to IIF modeling, the disadvantage of a phenomenological model is that it provides less insight into the mechanisms of IIF and the related injury to the cell. All

Received for publication 7 July 1993 and in final form 13 September 1993.

Address reprint requests to Dr. Mehmet Toner, Shriners Burns Institute, Research Center, One Kendall Square, Bldg 1400 W, Cambridge, MA 02142.

0006-3495/93/12/2524/13 $2.00

theoretical treatments of IIF presented in the literature to date have been concerned only with the onset of ice formation, and have neglected the subsequent growth phase of the ice crystals. The available IIF models are therefore adequate only for conditions under which the cell crystallizes instantly and completely upon the appearance of the first intracellular ice nucleus. However, empirical observations of "innocuous" intracellular crystallization indicate that the amount of ice formed in the cell is an important factor in determining the viability of frozen-thawed cells (Mazur, 1990; Rall et al., 1980; Borel Rinkes et al., 1992b). To predict the amount of ice formed in a cell, one must model the crystal growth process in the time-varying intracellular environment.

In this study, we present a model which describes nucleation and growth of ice crystals inside biological cells in the presence of the cryoprotectant dimethyl sulfoxide (DMSO), and apply this model to our recent experimental studies with cultured hepatocytes in the sandwich configuration (Borel Rinkes et al., 1992b). The model of Toner et al. (1990), has been extended to include the effect of CPAs, and intracellular ice growth has been modeled for the first time, using a modified version of the diffusion-limited crystal growth model of MacFarlane and Fragoulis (1986). In general, satisfactory agreement was obtained between the theoretical model predictions and published experimental observations. Correlation of predicted intracellular crystal volumes with previous measurements of cell damage allowed interpretation of the empirical findings in terms of the underlying physical processes, and provided some information about the amount of intracellular ice which causes irreversible damage in hepatocytes.

THEORETICAL BACKGROUND

A typical cell was modeled as a semipermeable membrane enclosing a solution of water, salt (NaCl), and DMSO (Fig.1). Also present in the cytoplasm are proteins and other large molecules, which are inactive with respect to all physical processes included in the model. For purposes of this investigation, the relevant control volume V_{cv} in the cell includes the cytosolic solution, but excludes the inactive cell volume V_b. The total cell volume is thus $V_{cell} = V_{cv} + V_b$. The cytoplasm temperature is assumed to be spatially uniform and is predetermined by the imposed cryopreservation protocol. The intracellular environment is also affected by exosmosis of water, which occurs in response to changing extracellular conditions during freezing.

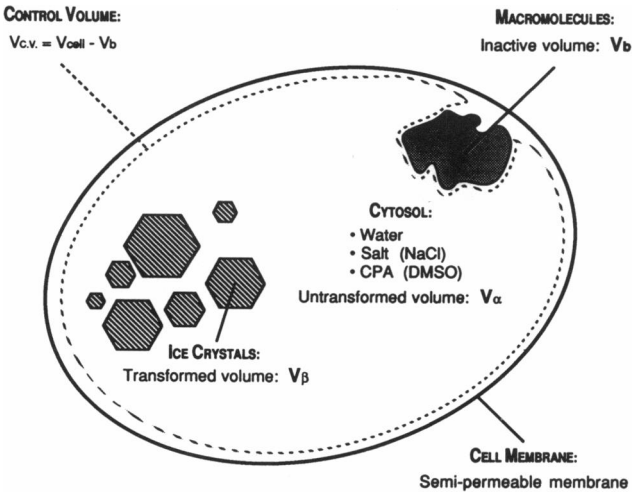

FIGURE 1 Schematic representation of the cell model.

To predict the amount of ice crystallization in the cell, equations describing nucleation and subsequent growth of ice have been coupled with a model describing the instantaneous state of the cytoplasm, i.e., its volume, solute concentrations, and temperature, as a function of time. The three-part, coupled model has been described in a theoretical study of homogeneous nucleation and crystal growth in mouse oocytes frozen in the presence of glycerol (Karlsson et al., submitted for publication). In the present work, this model has been modified for use with cultured hepatocytes frozen using DMSO as a cryoprotectant. The model has been extended further here by incorporating predictions of heterogeneous nucleation in the presence of DMSO. The important equations of the model are summarized below.

Kinetics of water transport

Transport across the cell membrane is driven by chemical potential differences between the intracellular and extracellular solutions. Because cell membranes are typically much more permeable to water than to CPA, and because the activation energy for water transport is larger than for CPA transport, the transport of CPA during freezing is assumed to be negligible compared with water transport. Although there is evidence suggesting that this assumption may not be valid during slow cooling (Diller and Lynch, 1984; Myers and Steponkus, 1986), there are no pertinent data for hepatocytes, and in the present study, changes in the cytosol composition during freezing were assumed to be determined entirely by the transport of water. Mazur (1963) developed a mathematical model for water transport, which has become the basis for all subsequent treatments. Model assumptions include membrane-limited transport, with negligible temperature and pressure differentials across the membrane, the external solution in equilibrium with extracellular ice, and an approximately ideal internal solution. Modifying this model to describe water transport for a ternary water-NaCl-DMSO system, one obtains the following differential equation:

$$\frac{dV_{cv}}{dt} = \frac{L_p \mathrm{ART}}{v_w}\left[\frac{\Delta H_f}{R}\left(\frac{1}{T_{mo}} - \frac{1}{T}\right) - \ln\left(\frac{V_{cv} - (n_s v_s + n_a v_a)}{V_{cv} - (n_s v_s + n_a v_a) + v_w(v_s n_s + n_a)}\right)\right] \quad (1)$$

where V_{cv} is the control volume as defined above; t, time; L_p, water permeability; A, membrane surface area; R, gas constant; T, temperature; ΔH_f, specific heat of fusion of water (assumed constant); T_{m0}, equilibrium melting point of water;

v_w, v_s, v_a, specific volumes of water, NaCl and DMSO, respectively; n_s, n_a, number of moles of NaCl and DMSO in the cell; and ν_s (=2), the dissociation constant of NaCl. Integration of Eq. 1 yields the data necessary to determine the state of the cytoplasm, i.e., the instantaneous values of V_{cv}, T, and the cytosol composition $\mathbf{c} = [c_w, c_s, c_a]$, where c_w, c_s, c_a are the intracellular concentrations of water, NaCl, and DMSO, respectively.

The membrane permeability L_p follows an Arrhenius temperature dependence:

$$L_p = L_{pg}(\mathbf{c})\exp\left[-\frac{E_{Lp}(\mathbf{c})}{R}\left(\frac{1}{T}-\frac{1}{T_{ref}}\right)\right] \quad (2)$$

where L_{pg} is the hydraulic permeability at the reference temperature T_{ref} = 273.15 K, and E_{Lp} is the activation energy for transport across the membrane. The values of L_{pg} and E_{Lp} have been measured for cultured hepatocytes under isotonic conditions in the absence of CPAs (Yarmush et al., 1992). The effect of CPAs on the membrane permeability can be estimated by reducing the value of L_{pg} by a factor of 0.5 for DMSO concentrations in excess of ~1 M (Mazur, 1990). There is still considerable disagreement concerning the magnitude of the effect of CPA on the value of E_{Lp}. Mazur (1990) presents evidence indicating that E_{Lp} may be independent of solution composition, whereas McCaa et al. (1991) report an increase in E_{Lp} for monocytes in the presence of DMSO. Inasmuch as measurements of the membrane permeability parameters for hepatocytes in the presence of CPAs are not available in the literature, E_{Lp} was left as an adjustable parameter in the model. Because the data of Borel-Rinkes et al. (1992b) suggest that IIF occurs in cultured hepatocytes frozen to −40°C in the presence of DMSO, when using a cooling rate of 16°C/min, E_{Lp} was chosen so that the predicted intracellular water content at −40°C for a cell cooled at 16°C/min would be sufficient to cause nucleation at this temperature. Fig. 2 shows the effect of the activation energy on the concentration of DMSO in the cell. DMSO concentrations are plotted as a function of temperature for a cooling rate of 16°C/min, for values of the activation energy ranging between 1.0 and 1.6 times the isotonic value. A factor of 1.55 was predicted to cause intracellular nucleation at −40°C, and this value was used in the rest of this study. This result is in reasonable agreement with the twofold increase in E_{Lp} measured by McCaa et al. (1991) for monocytes in 1 M DMSO. The numeric values of L_{pg} and E_{Lp} used in the water transport model are given in Table 1.

Intracellular ice nucleation

The rate of nucleation of intracellular ice crystals is a function of temperature and cytoplasm composition. In classical nucleation theory, a stable ice nucleus is formed by random clustering of water molecules. By assuming that clusters form by sequential addition of water monomers in a series of bimolecular reactions, and applying Eyring reaction rate theory to this process, the nucleation rate can be determined. For the homogeneous nucleation rate, J^{hom}, one obtains an expression of the form

$$J^{hom}(\mathbf{c}, T) = \Omega^{hom}(\mathbf{c}, T)\exp[-\kappa^{hom}(\mathbf{c}, T)T_m^5/T^3\Delta T^2] \quad (3)$$

where $\Delta T = (T_m - T)$ is the undercooling, T_m, the equilibrium melting point, and Ω^{hom} and κ^{hom}, the kinetic and thermodynamic coefficients, respectively (Turnbull and Fisher, 1949; Toner et al., 1990). J^{hom} gives the rate of formation of nuclei per unit volume of solution. The prefactor Ω^{hom} is directly proportional to the concentration of water monomers in the solution, and inversely proportional to the solution viscosity η. Given a viscosity model which predicts $\eta(\mathbf{c}, T)$, and the known reference value $\Omega o^{hom} = 9.7 \times 10^{52}$ m^{-3} s^{-1} for pure water (Kresin and Körber, 1991), the entire concentration and temperature dependence of $\Omega^{hom}(\mathbf{c}, T)$ can be obtained by scaling. The thermodynamic coefficient κ^{hom} depends on the ice-solution interfacial free energy σ. Because $\sigma(\mathbf{c}, T)$ is not known, $\kappa^{hom}(\mathbf{c}, T)$ has been estimated by requiring that Eq. 3 correctly predict observed homogeneous

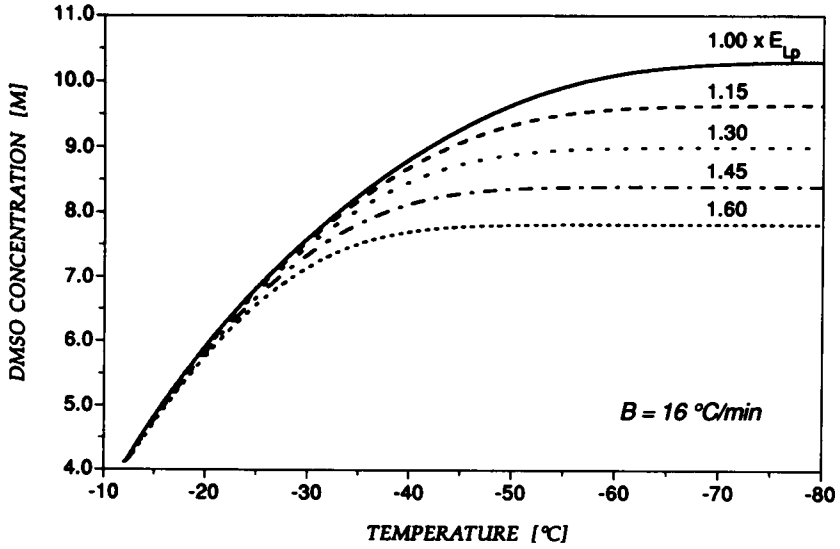

FIGURE 2 Sensitivity of predicted intracellular DMSO concentrations to variations in the activation energy for water transport. Labels indicate the magnitude of the activation energy relative to the isotonic value, E_{Lp} = 76.1 kJ/mol. The cooling rate was 16°C/min.

TABLE 1 Water transport model parameters for cultured hepatocytes

Parameter	Isotonic conditions	DMSO-treated cells*
V_{cell} (m^3)	5.0×10^{-15}	3.4×10^{-15} ‡
V_b (m^3)	2.6×10^{-15}	2.6×10^{-15}
A (m^2)	2.5×10^{-9}	2.5×10^{-9}
L_{pg} ($m\ s^{-1}\ Pa^{-1}$)	2.14×10^{-13}	1.07×10^{-13}
E_{Lp} ($J\ mol^{-1}$)	7.61×10^{4}	1.18×10^{5}
n_a (mol)	0	3.27×10^{-12}
n_s (mol)	3.50×10^{-13}	3.50×10^{-13}

* Cells equilibrated in 1.33 M DMSO.
‡ Value after isothermal hold at −12°C after seeding of external ice.

nucleation temperatures in solutions (Karlsson et al., submitted for publication; Rasmussen and MacKenzie, 1972).

Taking into account the effect of a catalytic substrate on the thermodynamics of cluster formation, an equation for the heterogeneous nucleation rate per unit substrate area, J^{het}, may be written as follows:

$$J^{het}(\mathbf{c}, T) = \Omega^{het}(\mathbf{c}, T)\exp[-\kappa^{het}(\mathbf{c}, T)T_m^5/T^3\Delta T^2] \quad (4)$$

where Ω^{het} and κ^{het} are the heterogeneous nucleation rate parameters. The theory of heterogeneous nucleation shows that the coefficients Ω^{het} and κ^{het} have the same basic functional forms as Ω^{hom} and κ^{hom}, with the effect of the catalytic substrate being described by a single additional parameter θ (Turnbull, 1950). Thus, the heterogeneous nucleation parameters can be calculated from the previous models for $\Omega^{hom}(\mathbf{c}, T)$ and $\kappa^{hom}(\mathbf{c}, T)$:

$$\Omega^{het}(\mathbf{c}, T) = \Omega_1^{het}(\mathbf{c}, T)\frac{\Omega^{hom}(\mathbf{c}, T)}{\Omega^{hom}(\mathbf{c}_1, T_1)}\left[\frac{f(\theta)}{f(\theta_1)}\right]^{1/6}$$
$$\kappa^{het}(\mathbf{c}, T) = \kappa_1^{het}(\mathbf{c}, T)\frac{\kappa^{hom}(\mathbf{c}, T)}{\kappa^{hom}(\mathbf{c}_1, T_1)}\frac{f(\theta)}{f(\theta_1)} \quad (5)$$

where $f(\theta)$ is the heterogeneous nucleation factor, ${\Omega_1}^{het}$ and ${\kappa_1}^{het}$ are known values of the kinetic and thermodynamic coefficients at a given concentration $\mathbf{c}_1$ and temperature T_1, and θ_1 is the corresponding value of θ. Reference nucleation rate parameters for heterogeneous nucleation were calculated from measurements of IIF in cultured hepatocytes frozen in 2 M DMSO at a cooling rate of 400°C/min (Hubel et al., 1991). Using a nonlinear regression analysis technique described elsewhere (Toner et al., 1990), the kinetic and thermodynamic coefficients were determined to be ${\Omega_1}^{het} = 4.5 \times 10^9\ m^{-2}\ s^{-1}$, ${\kappa_1}^{het} = 1.16 \times 10^{-3}$ (Fig. 3). The heterogeneous catalysis parameter $f(\theta)$ was assumed to remain approximately constant, thus $f(\theta)/f(\theta_1) \approx 1$. Fig. 4 shows the predicted nonequilibrium phase diagram for hepatocytes in 0.142 M NaCl and varying concentrations of DMSO, cooled at a constant rate of 400°C/min. In computing Fig.4, water transport was assumed negligible. Superimposed are nucleation temperature data from Hubel et al. (1991) for DMSO concentrations between 0 and 2 M. The predicted heterogeneous nucleation curve is in excellent agreement with the measured values, suggesting that the model assumptions are reasonable. Knowing the nucleation rates J^{hom} and J^{het}, one can calculate the instantaneous number of ice nuclei in the cell, $N(t)$, which in turn can be used to predict ice growth.

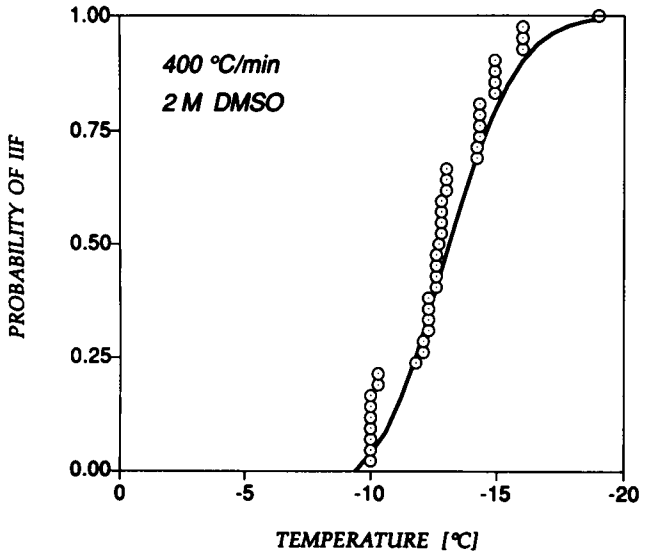

FIGURE 3 Determination of ${\Omega_1}^{het}$ and ${\kappa_1}^{het}$ by curve fitting of predicted IIF probabilities to measured probabilities of IIF in cultured hepatocytes frozen at 400°C/min in the presence of 2 M DMSO (data from Hubel et al., 1991). The best-fit curve ($\chi^2 \leq 10^{-4}$) is obtained for ${\Omega_1}^{het} = 4.5 \times 10^9\ m^{-2}\ s^{-1}$, ${\kappa_1}^{het} = 1.16 \times 10^{-3}$.

Diffusion-limited crystal growth

The rate of growth of ice crystals in the cytoplasm is assumed to be limited by the rate of diffusion of water molecules from the bulk solution to the crystal interface. MacFarlane and Fragoulis (1986) have developed a solution for nonisothermal, diffusion-limited growth, based on the theory presented by Christian (1975). Their results are adapted here for use in the present model. The crystals are assumed to be spherical, and sufficiently far apart that they do not interfere with each other (i.e., no impingement). Thus, far from the crystal, the concentration of water is spatially uniform, and its value c_∞ is determined by the water transport model. The solution adjacent to the crystal interface is assumed to be in thermal equilibrium with the ice, and the local water concentration is thus $c_{liq}(T)$, the liquidus concentration. For these conditions, the total crystallized volume can be shown to be

$$V^\beta(t) = \frac{4\pi}{3}\sum_{i=1}^{N(t)}\left[\int_{t_i}^{t}\alpha^2\bar{D}\,dt\right]^{3/2} \quad (6)$$

where the sum is taken over all nucleation instants t_i, and the nondimensional crystal growth parameter α is defined by

$$\alpha^3 = 2\frac{c_\infty - c_{liq}}{c_\beta - c_{liq}}\exp\left[-\frac{\alpha^2}{4}\right]\int_\alpha^\infty a^{-2}\exp\left[-\frac{a^2}{4}\right]da \quad (7)$$

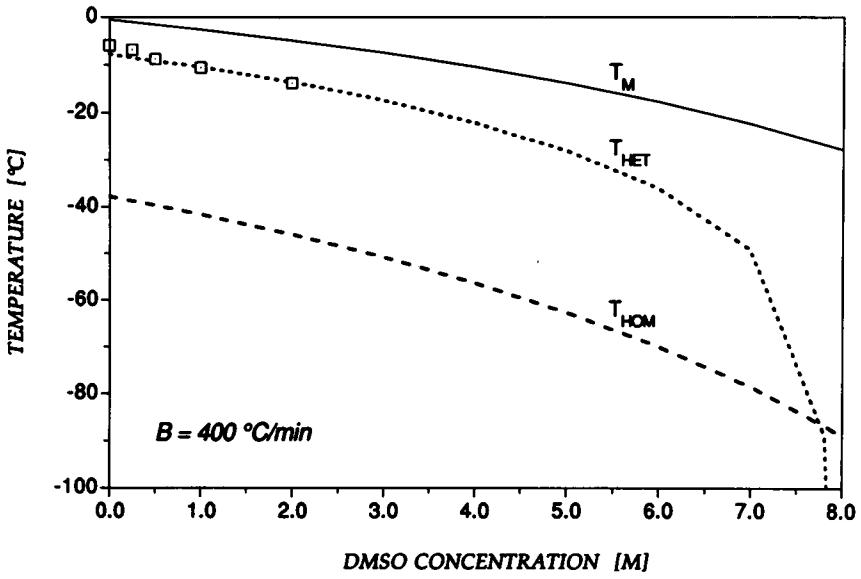

FIGURE 4 Predicted nonequilibrium phase diagram for cultured hepatocytes cooled at a rate of 400°C/min. T_m is the equilibrium freezing point, T_{het} the heterogeneous nucleation temperature, and T_{hom} the homogeneous nucleation temperature. The squares represent experimentally measured nucleation temperatures for cultured hepatocytes cooled at 400°C/min in various concentrations of DMSO (Hubel et al., 1991).

where c_β is the water concentration in ice (Christian, 1975). The effective diffusivity $\bar{D}$ is an average over the concentration range $c_{liq} < c_w < c_\infty$; the diffusivities at each individual water concentration were obtained from the viscosity model using the Stokes-Einstein relationship. Eq. 7 was solved numerically for α by iteration. To correct for impingement of multiple crystals growing in the same cell, Avrami's equation can be used (Christian, 1975):

$$X^\beta = 1 - \exp[-V^\beta/V_{cv}] \tag{8}$$

where X^β is the crystallized volume fraction. Avrami's correction is valid only for systems in which the solid and liquid phases have the same composition. Thus, the Avrami equation has limitations when applied to the ice growth in a ternary water-salt-DMSO solution, and the calculated X^β is primarily useful as an indicator of the extent of transformation of the intracellular water. For complete transformation ($X^\beta = 1$), the actual volume of ice in the cell is determined by the temperature and composition of the cytoplasm, and can be calculated from phase diagram information.

Viscosity estimation

Viscosity data for solutions of interest in cryobiology are scarce. Existing studies are typically limited to temperatures well above the equilibrium melting point, and relevant viscosity data for ternary water-salt-CPA solutions are virtually nonexistent. Cowie and Toporowski (1961) measured the concentration dependence of the viscosity of a binary water-DMSO system at 25°C. More recently, Eto et al. (1992) have obtained viscosity data down to −10°C for aqueous solutions of DMSO. These are the only such measurements available for subzero temperatures. Although they report best-fit Arrhenius parameters describing temperature dependence at several concentrations, more data are needed to establish conclusively the concentration dependence of the Arrhenius coefficients. For purposes of this study, a crude approximation to the function $\eta(\mathbf{c},T)$ has been constructed from the available data. Cowie and Toporowski's (1961) data were first fit with a polynomial

$$\eta_T(x_a) = 0.124\,x_a^6 - 0.452\,x_a^5 + 0.627\,x_a^4 - 0.391\,x_a^3 + 0.090\,x_a^2 + 0.004\,x_a + 0.001 \tag{9}$$

where η_T is the viscosity (in pascals-s) of a water-DMSO solution at 25°C for a given DMSO mole fraction x_a. The viscosity concentration dependence was assumed to have the same shape at any temperature, and thus the viscosity function $\eta_{DMSO}(x_a, T)$ for water-DMSO was obtained by scaling the curve $\eta_T(x_a)$ to fit the temperature dependence relationships measured by Eto and Rubinsky (1992). From their data for pure water (DMSO mole fraction $x_0 = 0$) and 8 M DMSO (mole fraction $x_1 = 0.25$):

$$\eta_{x_0}(T) = A_0 \exp[B_0/T]$$
$$\eta_{x_1}(T) = A_1 \exp[B_1/T] \tag{10}$$

scaling of $\eta_T(x_a)$ yields the desired function:

$$\eta_{DMSO}(x_a, T) = [\eta_T(x_a) - \eta_T(x_0)]\frac{\eta_{x_1}(T) - \eta_{x_0}(T)}{\eta_T(x_1) - \eta_T(x_0)} + \eta_{x_0}(T) \tag{11}$$

The viscosity of the ternary solution water-DMSO-NaCl was estimated by approximating the contribution from the salt particles using a hard-sphere model:

$$\eta(\mathbf{c}, T) = \eta_{DMSO}(\mathbf{c}, T)\exp\left[\frac{2.5\,\phi_s}{1 - Q\phi_s}\right] \tag{12}$$

where ϕ_s is the volume fraction of salt, and $Q = 0.609375$ is an interaction parameter (Vand, 1947). Although macromolecules and proteins may affect the viscosity of the intracellular solution, there are no experimental data on this interaction, and as a first approximation, the viscosity of the cytosol was assumed to be given by Eq. 12.

RESULTS

Numerical simulations

In the simulations presented here, the experimental freezing protocol used by Borel Rinkes et al. (1992b) is reproduced. The hepatocytes were initially equilibrated in a 1.33 M DMSO solution at 22°C and cooled down to −12°C at 10°C/min (Borel Rinkes et al., 1992a; 1992b). The cells were then partially dehydrated at −12°C by seeding external ice, and holding the cells at −12°C for 15 min (Borel Rinkes et al., 1992b). Solution of the water transport equation (Eq. 1) demonstrated that cells equilibrate completely by dehydration in less than ~10 s after the seeding of the external ice, and that during the remainder of the isothermal holding period, there is no driving force for transport of either water or DMSO. Assuming that during this initial ~10-s transient, the transport of solutes is negligible in comparison with the water efflux, one obtains a value for the new cell volume (V_{cell}) of 3.4×10^{-15} m^3, and intracellular solute concentrations of 4.12 M for DMSO and 0.44 M for NaCl. These values were used as initial conditions in the water transport simulations (Table 1). Simulations were run for the following freezing protocols: (1) freezing from −12°C to −40°C at constant cooling rates B (= $-dT/dt$) ranging between 1°C/min and 1000°C/min, followed by a 5-min isothermal holding period at −40°C, and (2) freezing from −12°C to various final temperatures between −40°C and −80°C, at various constant cooling rates. The corresponding temperature histories are shown in Fig. 5.

State of the cytoplasm

Figs. 6–9 describe the state of the cytoplasm during freezing from −12°C to −80°C at cooling rates ranging between 1°C/min and 1000°C/min. In Fig. 6, the intracellular water content, normalized to the value for isotonic conditions, is plotted against temperature. At the onset of constant rate cooling (T = −12°C), the hepatocytes contain only 22.6% of their original water volume, a consequence of the initial DMSO treatment and dehydration before freezing. The amount of water loss during cooling to −80°C is strongly dependent on the cooling rate. At slow cooling rates, dehydration is significant. For example, for a cooling rate of 1°C/min, only 4.1% of the intracellular water remains at −80°C. At fast rates, the final temperature of −80°C is reached before significant amount of water can be expressed. The final water content at a cooling rate of 1000°C/min is 21.0%, i.e., a loss of only 1.6% during cooling from −12°C to −80°C.

Figs. 7 and 8 show the intracellular concentrations of DMSO and NaCl, respectively, plotted versus temperature. Initially, the cells contain 4.12 M DMSO and 0.44 M NaCl; as the cells dehydrate during freezing, both salt and CPA concentrations increase, with slow cooling rates producing high intracellular solute concentrations, as expected. For a cooling rate of 1°C/min, the cytosol contains 9.5 M DMSO and 1.0 M NaCl at the final temperature of −80°C. However, if the same cell had been frozen with no DMSO present, the final intracellular salt concentration would have exceeded 21 M. Thus, the use of CPAs results in significant dilution of intracellular electrolytes. At fast cooling rates (≥400°C/min), the intracellular DMSO and NaCl concentrations do not change appreciably from their respective initial values.

In Fig. 9, the degree of undercooling, ΔT, of the cytoplasm is plotted as a function of temperature. At the onset of cooling at −12°C, the cells are in equilibrium with the external ice, and ΔT = 0. As the hepatocytes are cooled in the presence of ice, they express water to remain in equilibrium. The rate of water transport thus has a significant effect on the amount of undercooling observed in the cytosol. At a cooling rate of 400°C/min, the rate of water transport is practically negligible compared with the rate at which the cell temperature drops, and consequently no appreciable equilibration can occur. The resulting undercooling increases approximately linearly as the temperature decreases. At a cooling rate of 1°C/

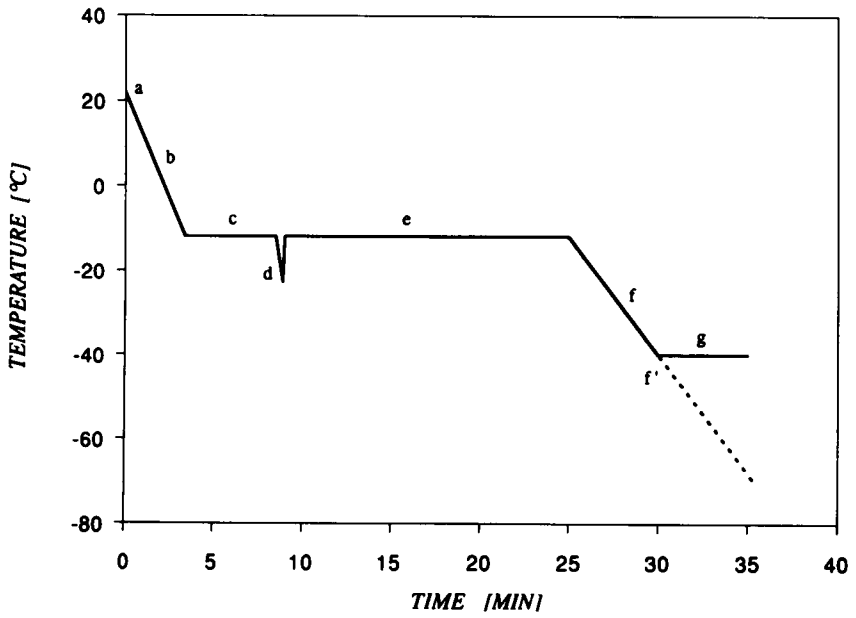

FIGURE 5 Freezing protocol used in simulations: (*a*) equilibration in 1.33 M DMSO at 22°C, (*b*) cooling to −12°C at 10°C/min, (*c*) thermal equilibration at −12°C, (*d*) seeding of external ice, (*e*) 15-min equilibration at −12°C, followed by either (*f*) cooling at various constant rates to −40°C and (*g*) 5-min isothermal holding period at −40°C, or (*f'*) cooling at various constant rates to various final temperatures between −12°C and −80°C.

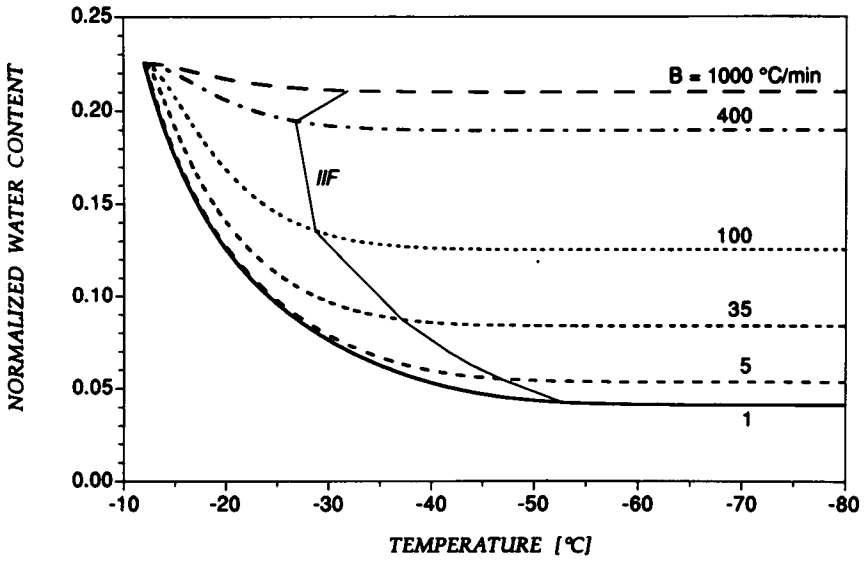

FIGURE 6 Predicted temperature dependence of the intracellular water content for cultured hepatocytes cooled at various constant rates. The normalized water content is defined as the water volume in the cell relative to the isotonic water volume, 2.5×10^{-15} m^3. The IIF-labeled curve indicates the predicted nucleation temperature for each cooling rate.

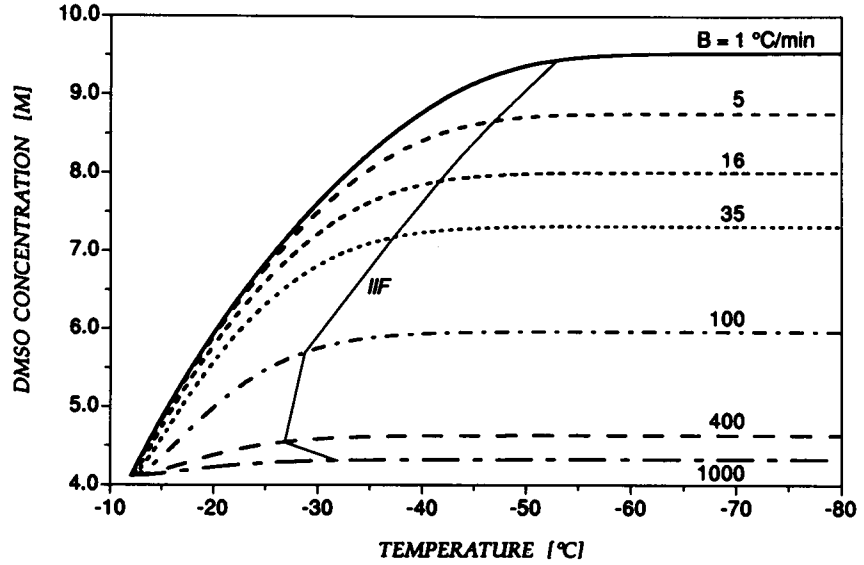

FIGURE 7 Predicted temperature dependence of the intracellular DMSO concentration for cultured hepatocytes cooled at various constant rates. The IIF-labeled curve indicates the predicted nucleation temperature for each cooling rate.

min, cooling is slow compared with the rate of removal of intracellular water, and the cytosol remains in equilibrium with the external ice (i.e., $\Delta T = 0$) for temperatures down to ~−30°C. However, at lower temperatures, one observes significant intracellular undercooling even at slow cooling rates, as a consequence of the Arrhenius temperature dependence of the membrane permeability (Eq. 2). The permeability L_p is reduced by about two orders-of-magnitude when the temperature falls from the initial temperature −12°C to −30°C. Thus, as the cell temperature decreases, the rate of water efflux decreases, and eventually a point is reached at which the water transport becomes negligible. This is clearly observed in Fig. 6, where the water content in the cell is seen to approach a constant value at temperatures below ~−40°C, even at very slow cooling rates. As a consequence of the drastically reduced membrane permeability, the cytoplasmic undercooling increases linearly as the cell temperature drops.

Nucleation and crystal growth

The number of intracellular ice nuclei N and the crystallized volume fraction X^β were predicted for cells cooled from −12°C to −40°C and then held at −40°C for 5 min to mimic experimental conditions (Borel Rinkes et al., 1992b). Table 2 shows the final values of N and X^β for various cooling rates, as well as the corresponding nucleation temperatures. The temperatures at which nucleation would occur if the cells were cooled further at the same rate, with no isothermal hold at −40°C, are also shown in parentheses for comparison purposes. Note that although a cell cooled continuously at a rate of 16°C/min would have a nucleation temperature of −41.6°C, the nucleation rate at −40°C is sufficiently high that a nucleus is formed during the 5-min isothermal hold at that temperature. For cooling rates less than 10°C/min, no nucleation was observed, and hence no crystal growth occurred in the cells. For cooling

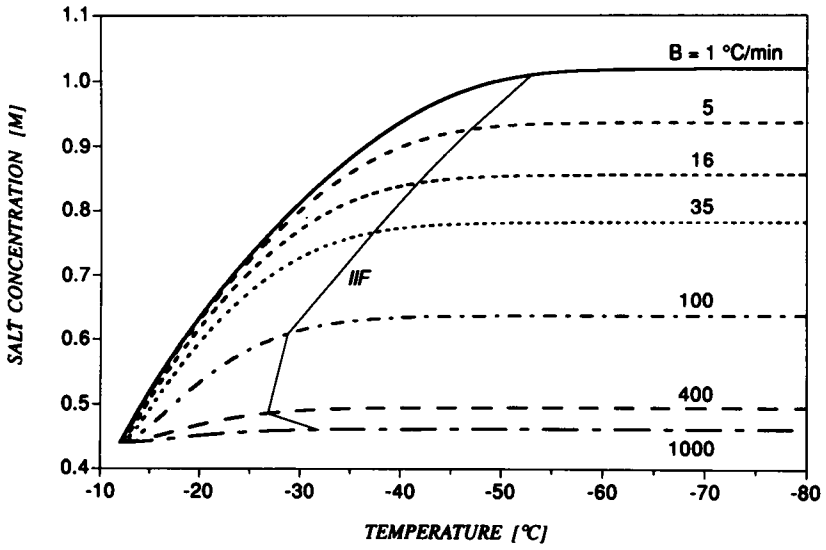

FIGURE 8 Predicted temperature dependence of the intracellular NaCl concentration for cultured hepatocytes cooled at various constant rates. The IIF-labeled curve indicates the predicted nucleation temperature for each cooling rate.

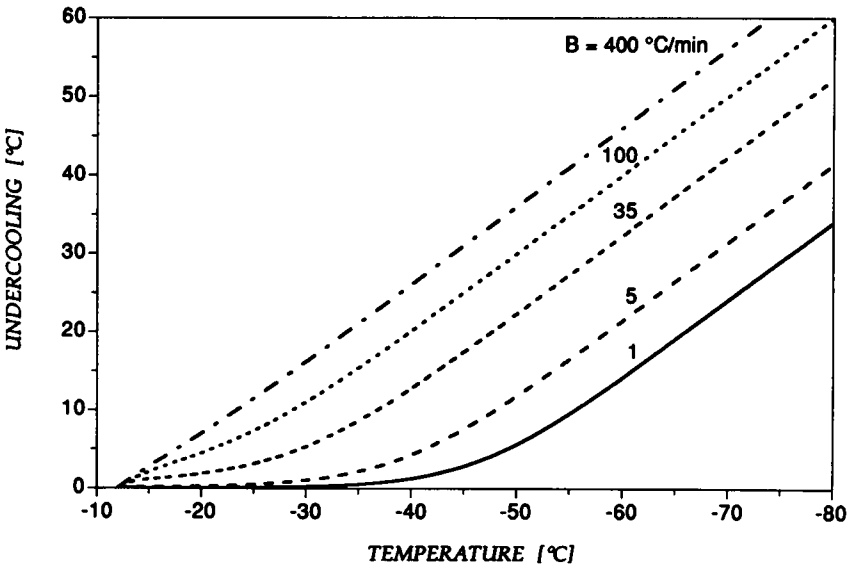

FIGURE 9 Predicted temperature dependence of the degree of intracellular undercooling for cultured hepatocytes cooled at various constant rates.

rates greater than 16°C/min, the intracellular water was completely transformed ($X^{\beta} = 1$) at the end of the freezing protocol at −40°C. The final number of nuclei was $N = 1$ for both 16°C/min and 35°C/min, i.e., the cell contained only a single ice crystal. Thus, for the conditions simulated, only mononuclear nucleation was observed. The final ice volume was calculated from the condition that the fully crystallized intracellular solution be at thermodynamic equilibrium and the assumption that water transport was negligible once nucleation had occurred. The resulting ice volumes, normalized to the total intracellular water volume under isotonic conditions, are shown in Fig. 10 as a function of the cooling rate. On the same figure, experimental albumin secretion data from Borel Rinkes et al. (1992b) are also shown for cultured hepatocytes subjected to the same freezing protocol simulated here, and subsequently thawed rapidly. The normalized albumin secretion (a measure of the differentiated function of the frozen-thawed hepatocyte cultures) has a maximum between cooling rates of 5°C/min and 10°C/min, corresponding to the optimal cooling rate. At suboptimal cooling rates, albumin

TABLE 2 Predicted nucleation temperature, final number of ice nuclei, and final crystallized volume fraction in cultured hepatocytes cooled to −40°C at the given cooling rate, then held isothermally at −40°C for 5 min

B (°C/min)	T_{het} (°C)	N_{final}	$X^{\beta_{final}}$
1	– (−52.9)*	0	0.0
5	– (−46.8)	0	0.0
10	– (−43.8)	0	0.0
16	−40.0 (−41.6)	1	1.0
35	−37.2 (−37.2)	1	1.0

* Nucleation temperatures for cells cooled continuously at the given rate, with no isothermal hold at −40°C.

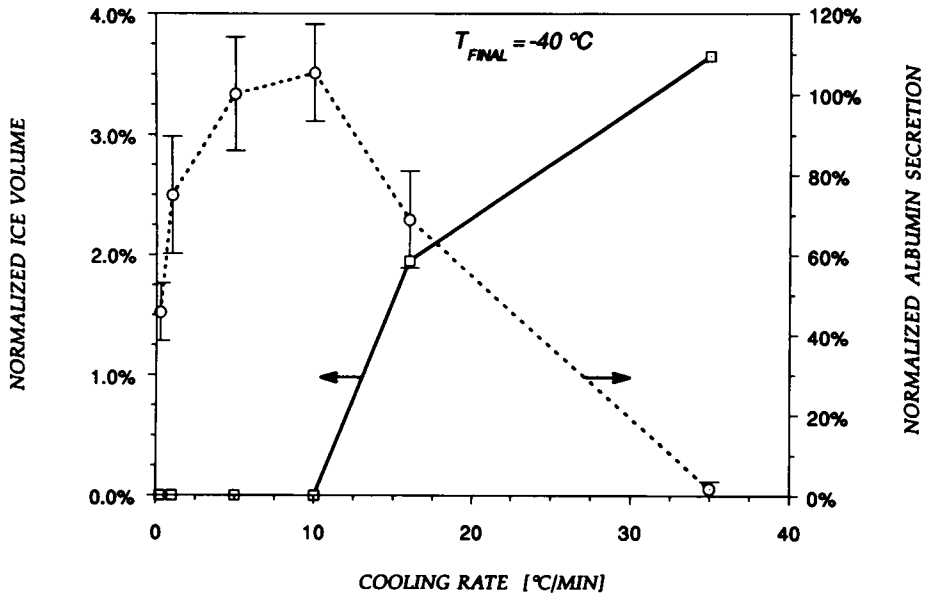

FIGURE 10 Effect of cooling rate on predicted intracellular ice content and measured albumin secretion levels for cultured hepatocytes cooled to a final temperature of −40°C, then held isothermally at −40°C for 5 min before rewarming. The normalized ice volume (*solid line*) is the predicted amount of intracellular ice at the end of the isothermal hold, relative to the isotonic water volume, 2.5×10^{-15} m^3. The albumin secretion data (*broken line*) are from Borel Rinkes et al. (1992b).

secretion decreases with decreasing cooling rate; at supraoptimal cooling rates, the albumin secretion drops with increasing cooling rate. A comparison of these results with the predicted intracellular ice volume as a function of cooling rate shows that at or below the optimal cooling rate, there is no crystal growth in the cells, whereas for supraoptimal rates the amount of intracellular ice increases with increasing cooling rate. Thus, the level of albumin secretion, and therefore hepatocyte viability, correlates inversely with the intracellular ice volume at supraoptimal rates. The drop in viability at suboptimal rates, where no crystallization occurs, is commonly ascribed to "solution effects" not pertaining to IIF, i.e., damage related to high intracellular and extracellular solute concentrations, excessive cell shrinkage, mechanical deformation, or other forces (Mazur, 1984).

In addition to the dependence of crystal growth and corresponding cell viability on cooling rate, their dependence on the final freezing temperature was also investigated. In Fig. 11, the predicted crystallized volume fraction X^β is plotted

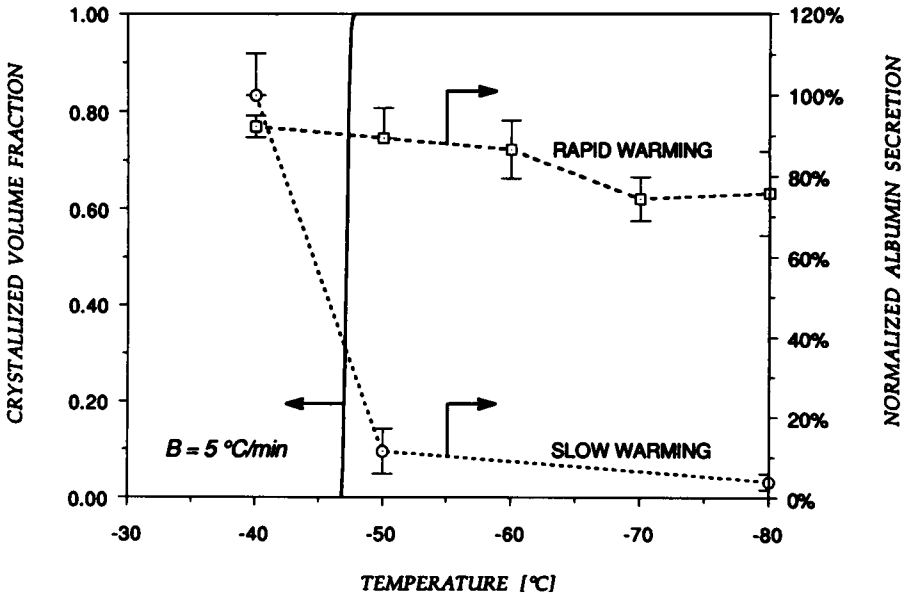

FIGURE 11 Effect of the final freezing temperature on the predicted crystallized volume fraction (*solid line*) and on measured albumin secretion levels (*broken lines*) for cultured hepatocytes cooled at a rate of 5°C/min. The albumin secretion data are for cells cooled to the given final temperature, held isothermally at the final temperature for 5 min, then rewarmed either rapidly (≥400°C/min) or slowly (5°C/min) (Borel Rinkes et al., 1992b).

as a function of temperature for a cell cooled at 5°C/min down to −80°C. Shown on the same plot are albumin secretion data for hepatocyte cultures frozen at a cooling rate of 5°C/min to various final temperatures between −40°C and −80°C, and rewarmed either rapidly (≥400°C/min) or slowly (5°C/min) after a 5-min isothermal hold at the selected final temperature (Borel Rinkes et al., 1992b). As can be seen from the X^β curve, intracellular ice nucleates at −46.8°C, followed by a very rapid transition from $X^\beta = 0$ to $X^\beta = 1$. The normalized albumin secretion measured after slow thawing is ~100% for a final hold temperature of −40°C, and drops to a value of less than 10% when the final freezing temperature is less than −50°C. This drastic reduction in protein secretion correlates well with the predicted nucleation temperature. For rapid warming rates, the measured albumin secretion remains at approximately normal levels, decreasing only slightly to ~80% as the final freezing temperature is decreased. Since the model predicts formation of intracellular ice when hepatocytes are frozen to −50°C or lower, these data suggest that the intracellular crystallization during the specified freezing protocol is innocuous, and that the damage in slowly warmed cells occurs during thawing.

Ice nucleation temperatures were also calculated for freezing at cooling rates other than 5°C/min. These are shown on Fig. 6 (*curve IIF*) superimposed on the corresponding water content curve for each cooling rate. For a given cooling rate, nucleation occurs when the water content curve crosses the IIF curve (i.e., when the nucleation temperature is reached). IIF curves have also been drawn in Figs. 7 and 8, showing the dependence of the nucleation temperature on the intracellular solute concentrations. At cooling rates below 400°C/min, the intracellular nucleation temperature is depressed as the cooling rate decreases because of the corresponding increase in the intracellular solute concentration. However, the nucleation temperature is also lowered when the cooling rate increases from a cooling rate of 400°C/min to 1000°C/min. At these high cooling rates, cell dehydration is negligible, and therefore the nucleation rate is independent of the rate of cooling. The observed depression in the temperature of nucleation is a kinetic effect, i.e., in the time required to form a stable nucleus at a given nucleation rate, a significant temperature drop can be achieved at very fast cooling rates.

DISCUSSION

This work describes a theoretical model of IIF in which water transport predictions are coupled with physicochemical models of nucleation and growth of ice crystals. The model of intracellular heterogeneous nucleation in the absence of CPAs, developed by Toner et al. (1990), has been extended to include the effect of CPAs on the nucleation process. In addition, predictions of the crystal growth kinetics of intracellular ice have been incorporated into the model, by modifying the crystal growth theory of MacFarlane and Fragoulis (1986). The model has then been applied to prior data obtained on the freezing of cultured hepatocytes in the presence of DMSO (Borel Rinkes et al., 1992b) to better understand the mechanisms underlying the empirical observations. The model predictions were in good agreement with the experimental data, and provide important physical insight into the processes relevant to cryopreservation of cultured hepatocytes.

Nonequilibrium phase diagram

Heterogeneous nucleation temperatures for cultured hepatocytes have been predicted for the first time as a function of DMSO concentration; using these data, a nonequilibrium phase diagram could be constructed (Fig. 4). For DMSO concentrations less than ~3 M, the predicted heterogeneous nucleation temperature curve was found to be approximately parallel to the liquidus curve ($\Delta T_{het} \approx 1.3\Delta T_m$). This finding is consistent with the empirical results of Reischel and Vali (1975). For hepatocytes, the heterogeneous nucleation curve lies only 7–10°C below the liquidus, and thus only limited undercooling is allowed in the cells if IIF is to be avoided. The implication is that to prevent completely the nucleation of ice crystals inside cultured hepatocytes, one must either cool at extremely slow rates (i.e., much less than 1°C/min; see Fig. 6) to maintain near-equilibrium conditions, or use high concentrations of CPA to depress the equilibrium freezing temperature to a point approaching the final storage temperature. In both cases, the cells are exposed to high CPA concentrations, which may be deleterious. An alternative, and more appropriate strategy for cryopreservation of sandwich-cultured hepatocytes, might be to permit intracellular nucleation to occur, but to limit the extent of crystal growth in the cell to an innocuous level by expressing enough of the intracellular water during cooling.

At high DMSO concentrations, the predicted heterogeneous nucleation temperature begins to drop sharply as the CPA content increases, and at DMSO concentrations higher than 7.8 M, homogeneous nucleation becomes the dominant mechanism of nucleation. Rall et al. (1983) have observed such a transition from a heterogeneous to a homogeneous mechanism of intracellular nucleation in eight-cell mouse embryos frozen in the presence of DMSO or glycerol. Mouse embryos were found to nucleate by a homogeneous mechanism when CPAs were present in concentrations of 1.5 M or higher. These results suggest that CPAs have a much more pronounced effect on IIF temperatures for mouse embryos than for cultured hepatocytes. Although the shape and location of the homogeneous nucleation curve on the phase diagram depends only on the nature of the freezing solution, the heterogeneous nucleation curve is highly dependent on cell type and the specific mechanism of catalysis. The shape of the heterogeneous nucleation curve is thus of major importance in selecting strategies for cryopreservation.

Kinetics of water transport

The trajectory of the cytosol through its state-space is determined by the kinetics of water transport out of the cell. The main difficulty of accurately predicting water transport is the measurement of the membrane permeability parameters L_{pg} and E_{Lp} under conditions relevant to cryopreservation, i.e.,

at subzero temperatures and in the presence of various concentrations of CPA and other solutes. Although the permeability parameters for cultured hepatocytes under isotonic conditions have recently been measured at subzero temperatures (Yarmush et al., 1992), the CPA dependence of these parameters remains unknown. In the present work, the value of the activation energy E_{Lp} has been adjusted to yield plausible predictions of intracellular water content. Reasonable results were obtained if E_{Lp} increased by a factor of 1.55 in the presence of DMSO. Although this value is in concordance with existing experimental evidence (McCaa et al., 1991), it is clear that direct measurements of the membrane permeability parameters are needed. It should also be noted that the transport of CPA during freezing has been neglected in this study. The assumption that CPA transport is negligible during freezing is justified for sufficiently rapid rates of cooling, but some CPA permeation may occur at very slow cooling rates. However, the main focus of the present work is on cooling rates sufficiently fast to cause IIF (i.e., >10°C/min, see Fig. 10), at which CPA permeation is probably insignificant.

The water transport simulations reveal that, as a result of the Arrhenius dependence of the membrane permeability, the cell becomes quasiimpermeable at low temperatures, effectively trapping the remaining water inside the cell. Hence, even at very slow cooling rates the cytoplasm will eventually become significantly undercooled, ultimately undergoing IIF. When hepatocytes were cooled to −80°C, intracellular ice nucleated at all simulated cooling rates between 1°C/min and 1000°C/min. Conceivably, extremely slow cooling rates (much less than 1°C/min) could be used to depress the nucleation temperature to below the final storage temperature, thus completely avoiding IIF. However, hepatocytes were found to experience damage due to "solution effects" at cooling rates less than 1°C/min (IIF could be eliminated as a possible cause of the observed cell injury at these slow cooling rates, because cooling was interrupted at −40°C, well above the nucleation temperature). For cooling rates sufficiently fast to avoid damage by solution effects, nucleation always occurred at temperatures higher than −50°C. Thus, when hepatocytes are frozen to temperatures below this value, intracellular crystallization is inevitable. The viability of the cells will therefore be a function of the extent of intracellular crystallization: if the amount of ice formed during freezing is sufficiently low, the cells can be "rescued" by rapid warming. However, if the rate of rewarming is too slow, the intracellular crystals can grow to damaging proportions during warming. Because hepatocytes were predicted to undergo IIF at all cooling rates, rapid rewarming rates were always required to prevent injury during the thawing process.

Intracellular crystal growth

The quantification of the permissible amount of intracellular ice is a problem of critical importance to cryobiology. Progress toward resolving this question has been hampered by the previous lack of a fundamental theoretical treatment of intracellular crystal growth, as well as the paucity of relevant experimental data. Mazur (1990) estimates that mouse ova containing ≤16% of their isotonic water volume upon IIF will be "rescuable," but notes that the value of this limit seems to vary for different CPA concentrations. Shimada (1977) indicated that ice crystals smaller than ~0.05 μm are innocuous to HeLa cells. To provide a better understanding of damage by intracellular ice in hepatocytes, and to attempt to define what may constitute innocuous crystallization, the crystal growth predictions of the present study have been correlated with existing viability measurements (Borel Rinkes et al., 1992b). The intracellular ice volume was predicted to increase with increasing cooling rate, a consequence of the high water content in cells which are frozen rapidly. For cooling rates faster than ~5°C/min, the predicted equilibrium ice volume in the cell was thus found to be positively correlated with the loss of function in hepatocytes, suggesting a link between cell damage and intracellular ice volume for this range of cooling rates.

Quantitative comparison of crystal growth predictions with measurements of cell viability provides useful information regarding the conditions under which intracellular ice can be considered innocuous. Even though IIF is predicted to occur when cells are frozen at a cooling rate of 16°C/min, albumin secretion levels remain at almost 70% of normal values, indicating that the intracellular ice crystals inflicted only partial damage on the hepatocyte culture. At this cooling rate, the cell nucleates with 7.0% of its isotonic water volume remaining, which in equilibrium at −40°C yields a normalized ice volume of only 2.0% (Fig. 10). Hepatocytes, frozen at a cooling rate of 35°C/min, on the other hand, experience total loss of function. The corresponding intracellular water content at the nucleation temperature (−37.2°C) is 8.7%, which when fully frozen at −40°C results in a crystal volume of 3.7% relative to the total isotonic water volume. Therefore, based on the model predictions, the critical ice volume causing irreversible damage in hepatocytes appears to lie in the range of 2.0% to 3.7%.

The results of the above analysis should be interpreted with the caveat that crystal growth velocities may have been overestimated at low temperatures, due to uncertainties in the phenomenological model used to determine the cytosol viscosity. If the rate of crystal growth under the experimental conditions was sufficiently slow to partially vitrify the cell ($X^{\beta} < 1$), then the actual intracellular ice volumes may have been considerably lower than the predicted equilibrium values given above. Nonetheless, 3.7% would still represent an upper bound to the critical intracellular ice volume. Problems with the viscosity model stem from the fact that it was constructed by extrapolation of measurements made above −10°C. Furthermore, the Arrhenius temperature dependence employed in the viscosity model precludes the typically drastic viscosity increase near the glass transition temperature observed for many glass-forming solutions. Further experimental work to measure the viscosity of water-DMSO solutions at low temperatures is clearly necessary.

The model predictions for cells frozen at a cooling rate of 5°C/min to −80°C (Fig. 11) provide further evidence that innocuous crystallization can occur in hepatocytes, and successfully explain the measured dependence of hepatocyte function on the final freezing temperature and on warming rate. Cells frozen to −40°C at 5°C/min remain above the predicted nucleation temperature of −46.8°C, and are thus not damaged by intracellular ice, either during freezing or subsequent rewarming. Consequently, the survival is independent of warming rate. However, for final freezing temperatures lower than −50°C, total loss of function is observed in hepatocytes which were warmed slowly, whereas rapidly warmed cells retain protein secretion levels close to normal. Because −50°C lies below the calculated nucleation temperature (−46.8°C), ice should be present in the cell. Because cells which were warmed rapidly appear to be undamaged, these ice crystals must be innocuous. However, if slow warming rates are used, the crystals can grow to sizes which are damaging to the cell; hence, the sharp drop-off in survival coincident with the initial appearance of an ice nucleus in the cytoplasm. In contrast, at rapid warming rates, there is no further growth of the intracellular ice crystals which form during freezing, and thus the cells remain viable.

Because ice formation in cultured hepatocytes frozen at 5°C/min to −80°C is innocuous, the corresponding normalized ice volume must be less than 3.7%, the calculated upper bound to the critical ice volume. However, the intracellular water content at the nucleation temperature for cells cooled at 5°C/min is 5.5% of isotonic, which fully frozen at −80°C would yield a normalized ice volume of 4.0%. Hence, one may conclude that hepatocytes frozen at 5°C/min to −80°C partially vitrify, i.e., that the final intracellular ice volume is less than the equilibrium value. Vitrification has been observed experimentally in mouse embryos cooled rapidly in the presence of 4.5 M DMSO and 0.25 M sucrose (Li and Trounson, 1991), and glycerol solutions have been vitrified independent of cooling rate at concentrations of ~7 M (Fahy et al., 1984). Compared with the predicted intracellular DMSO content of 8.7 M at the nucleation temperature for hepatocytes cooled at a rate of 5°C/min, these data support the conclusion that the hepatocytes vitrify under the given conditions.

CONCLUSION

The integrated water transport, nucleation, and crystal growth model developed in this study has been applied with considerable success to cultured hepatocytes frozen in the presence of DMSO. The model predicts and explains the dependencies of the function of cultured hepatocytes on cooling rate, warming rate, and final freezing temperature. Cell damage was found to correlate positively the amount of intracellular ice crystallized, but inadequacies of the viscosity model precluded the determination of the exact value of the critical ice volume, below which intracellular ice crystals are innocuous. The major weaknesses of the model were found to be the estimates of the model parameters. Determination of the membrane permeability activation energy, E_{Lp}, and the cytosol viscosity, η, as functions of concentration and temperature was especially problematic, and better measurements of these parameters at low temperatures are necessary. The fundamental quantitative understanding gained in this study using cultured rat hepatocytes needs to be extended to cultured human hepatocytes. Further application of this model to isolated hepatocytes is also crucial for the successful clinical implementation of bioartificial liver devices.

This research was supported in part by the Edward Hood Taplin Professorship in Medical Engineering, the National Institutes of Health (1R29 DK 46270), the Whitaker Foundation (to M. T.), and the Shriners Hospital for Crippled Children.

REFERENCES

Borel Rinkes, I. H. M., M. Toner, R. M. Ezzel, R. G. Tompkins, and M. L. Yarmush. 1992a. Effects of dimethyl sulfoxide on cultured rat hepatocytes in sandwich configuration. *Cryobiology*. 29:443–453.

Borel Rinkes, I. H. M., M. Toner, S. J. Sheehan, R. G. Tompkins, and M. L. Yarmush. 1992b. Long-term functional recovery of hepatocytes after cryopreservation in a three-dimensional culture configuration. *Cell Transplantation*. 1:281–292.

Chesné, C., and A. Guillouzo. 1988. Cryopreservation of isolated rat hepatocytes: a critical evaluation of freezing and thawing conditions. *Cryobiology*. 25:323–330.

Christian, J. W. 1975. The Theory of Transformation in Metals and Alloys. Pergamon, New York. p 418.

Cowie, J. M. G., and P. M. Toporowski. 1961. Association in the binary liquid system dimethyl sulfoxide-water. *Can. J. Chem.* 39:2240–2243.

Diller, K. R., and M. E. Lynch. 1984. An irreversible thermodynamic analysis of cell freezing in the presence of membrane-permeable additives. II. Transient electrolyte and additive concentrations. *Cryo Lett.* 5:117–130.

Eto, T. K., B. Rubinsky, B. J. Costello, S. W. Wenzel, and R. M. White. 1992. Lamb wave microsensor measurement of viscosity as a function of temperature of dimethylsulfoxide solutions. *In* Topics in Heat Transfer. M. Toner, M. I. Flik, B. W. Webb, D. T. Vader, R. V. Arimilli, H. J. Sauer, J. Georgiadis, V. Prasad, editors. Vol. 206–2. American Society of Mechanical Engineers, New York, 47–53.

Fahy, G. M., D. R. MacFarlane, C. A. Angell, and H. T. Meryman. 1984. Vitrification as an approach to cryopreservation. *Cryobiology*. 21: 407–426.

Fuller, B. J., J. Lewin, and L. Sage. 1983. Ultrastructural assessment of cryopreserved hepatocytes after prolonged ectopic transplantation. *Transplantation (Baltimore)*. 35:15–18.

Gomez-L., M. J., P. Lopez, and J. V. Castell. 1984. Biochemical functionality and recovery of hepatocytes after deep freezing storage. *In Vitro (Rockville)*. 20:826–832.

Hubel, A., M. Toner, E. G. Cravalho, M. L. Yarmush, and R. G. Tompkins. 1991. Intracellular ice formation during the freezing of hepatocytes cultured in a double collagen gel. *Biotechnol. Prog.* 7:554–559.

Innes, G. K., B. J. Fuller, and K. E. F. Hobbs. 1988. Functional testing of hepatocytes following their recovery from cryopreservation. *Cryobiology*. 25:23–30.

Kresin, M., and C. Körber. 1991. Influence of additives on crystallization kinetics: comparison between theory and measurements in aqueous solutions. *J. Chem. Phys.* 95:5249–5255.

Li, R., and A. Trounson. 1991. Rapid freezing of the mouse blastocyst: effects of cryoprotectants and of time and temperature of exposure to cryoprotectant before direct plunging into liquid nitrogen. *Reprod. Fertil. Dev.* 3:175–183.

MacFarlane, D. R., and M. Fragoulis. 1986. Theory of devitrification in multicomponent glass forming systems under diffusion control. *Phys. Chem. Glasses*. 27:288–234.

Mazur, P. 1963. Kinetics of water loss from cells at subzero temperatures and the likelihood freezing. *J. Gen. Physiol.* 47:347–369.

Mazur, P. 1984. Freezing of living cells: mechanisms and implications. *Am. J. Physiol.* 143:C125-C142.

Mazur, P. 1990. Equilibrium, quasi-equilibrium, and nonequilibrium freezing of mammalian embryos. *Cell Biophys.* 17:53–92.

McCaa, C., K. R. Diller, S. J. Aggarwal, and T. Takahashi. 1991. Cryomicroscopic determination of the membrane osmotic properties of human monocytes at subfreezing temperatures. *Cryobiology.* 28:391–399.

Myers, S. P., and P. L. Steponkus. 1986. Permeation of dimethyl sulfoxide into rye protoplasts during freezing of the suspending medium. *Cryo Lett.* 7:41–54.

Novicki, D. L., G. P. Irons, S. C. Strom, R. Jirtle, and G. Michalopoulos. 1982. Cryopreservation of isolated rat hepatocytes. *In Vitro (Rockville).* 18:393–399.

Pitt, R. E. 1992. Thermodynamics and intracellular ice formation. *In* Advances in Low-Temperature Biology. Vol. 1. P. L. Steponkus, editor. J. A. I. Press Ltd., London. 63–99.

Rall, W. F., P. Mazur, and J. J. McGrath. 1983. Depression of the ice-nucleation temperature of rapidly cooled mouse embryos by glycerol and dimethyl sulfoxide. *Biophys. J.* 41:1–12.

Rall, W. F., D. S. Reid, and J. Farrant. 1980. Innocuous biological freezing during warming. *Nature (Lond.).* 286:511–514.

Rasmussen, D. H., and A. P. MacKenzie. 1972. Effect of solute on ice-solution interfacial free energy calculation from measured homogeneous nucleation temperatures. *In* Water Structure at the Water-Polymer Interface. H. H. G. Jellinek, editor. Plenum Press, New York. 126–145.

Reischel, M. T., and G. Vali. 1975. Freezing nucleation in aqueous electrolytes. *Tellus.* 27:414–426.

Rijntjes, P. J. M., H. J. Moshage, P. J. L. van Gemert, R. de Waal, and S. H. Yap. 1986. Cryopreservation of adult human hepatocytes. The influence of deep freezing storage on the bioability, cell seeding, survival, fine structures, and albumin synthesis in primary cultures. *J. Hepatol. (Amst.).* 3:7–18.

Shimada, K. 1977. Effects of cryoprotective additives on intracellular ice formation and survival in very rapidly cooled HeLa cells. *Contrib. Inst. Low Temp. Sci. Hokkaido Univ. Ser. B.* 19:49–69.

Toner, M., E. G. Cravalho, and M. Karel. 1990. Thermodynamics and kinetics of intracellular ice formation during freezing of biological cells. *J. Appl. Phys.* 67:1582–1593. *Erratum:* 1991. *J. Appl. Physiol.* 10:4653.

Toner, M., E. G. Cravalho, J. Stachecki, T. Fitzgerald, R. G. Tompkins, M. L. Yarmush, and D. R. Armant. 1993. Nonequilibrium freezing of one-cell mouse embryos. *Biophys. J.* 64:1908–1921.

Toner, M., R. G. Tompkins, E. G. Cravalho, and M. L. Yarmush. 1992. Transport phenomena during freezing of isolated hepatocytes. *Am. Inst. Chem. Eng. J.* 38:1512–1522.

Turnbull, D. 1950. Kinetics of heterogeneous nucleation. *J. Chem. Phys.* 18:198–203.

Turnbull, D., and J. C. Fisher. 1949. Rate of nucleation in condensed systems. *J. Chem. Phys.* 17:71–72.

Vand, V. 1947. Viscosity of Solutions and Suspensions. I. *J. Phys. Chem.* 52:277–299.

Yarmush, M. L., M. Toner, J. C. Y. Dunn, A. Rotem, A. Hubel, and R. G. Tompkins. 1992. Hepatic tissue engineering: development of critical technologies. *Ann. N. Y. Acad. Sci.* 665:238–252.